

Viscoelastic properties of individual glial cells and neurons in the CNS

Yun-Bi Lu^{†‡§}, Kristian Franze^{‡§}, Gerald Seifert[¶], Christian Steinhäuser[¶], Frank Kirchhoff[¶], Hartwig Wolburg^{††}, Jochen Guck[§], Paul Janmey^{††}, Er-Qing Wei[†], Josef Käs^{‡§§}, and Andreas Reichenbach[‡]

[†]Department of Pharmacology, School of Medicine, Zhejiang University, Yan An Road 353, Hangzhou 310031, China; [‡]Paul Flechsig Institute of Brain Research, Universität Leipzig, Jahnallee 59, 04109 Leipzig, Germany; [§]Division of Soft Matter Physics, Department of Physics, Universität Leipzig, Linnéstrasse 5, 04103 Leipzig, Germany; [¶]Institute of Cellular Neurosciences, Universität Bonn, Sigmund-Freud-Strasse 25, 53105 Bonn, Germany; ^{¶¶}Department of Neurogenetics, Max Planck Institute of Experimental Medicine, Hermann-Rein-Strasse 3, 37075 Göttingen, Germany; ^{††}Institute of Pathology, Universität Tübingen, Liebermeisterstrasse 8, 72076 Tübingen, Germany; and ^{‡‡}Institute for Medicine and Engineering, University of Pennsylvania, 1010 Vagelos Laboratories, 3340 Smith Walk, Philadelphia, PA 19104

Edited by Harry L. Swinney, University of Texas, Austin, TX, and approved September 28, 2006 (received for review July 21, 2006)

One hundred fifty years ago glial cells were discovered as a second, non-neuronal, cell type in the central nervous system. To ascribe a function to these new, enigmatic cells, it was suggested that they either glue the neurons together (the Greek word “γλῖα” means “glue”) or provide a robust scaffold for them (“support cells”). Although both speculations are still widely accepted, they would actually require quite different mechanical cell properties, and neither one has ever been confirmed experimentally. We investigated the biomechanics of CNS tissue and acutely isolated individual neurons and glial cells from mammalian brain (hippocampus) and retina. Scanning force microscopy, bulk rheology, and optically induced deformation were used to determine their viscoelastic characteristics. We found that (i) in all CNS cells the elastic behavior dominates over the viscous behavior, (ii) in distinct cell compartments, such as soma and cell processes, the mechanical properties differ, most likely because of the unequal local distribution of cell organelles, (iii) in comparison to most other eukaryotic cells, both neurons and glial cells are very soft (“rubber elastic”), and (iv) intriguingly, glial cells are even softer than their neighboring neurons. Our results indicate that glial cells can neither serve as structural support cells (as they are too soft) nor as glue (because restoring forces are dominant) for neurons. Nevertheless, from a structural perspective they might act as soft, compliant embedding for neurons, protecting them in case of mechanical trauma, and also as a soft substrate required for neurite growth and facilitating neuronal plasticity.

biomechanics | elasticity | viscosity | retina | hippocampus

In his search for a “connective tissue” in the brain, the pathologist Rudolf Virchow (1) discovered a non-neuronal cell type that he termed glial cells (“Nervenkitt”), stemming from his designation of their function as a glue or putty for the already known neurons. Another equally prominent historic view implies that glial cells provide a supportive scaffold (“Stützzellen”) to which the neurons are attached like Christmas ornaments to a tree (2). Motivated by this perspective the term “support cells,” support as in structural support, is generally used for glial cells of sensory organs such as the retina.

To recognize the difference in these two viewpoints, one needs to envisage that putty at the times of Virchow was rather soft and viscous (i.e., nonelastic), similar to honey, whereas the term support cell implies glial cells to be stiff and dominantly elastic elements like the piers of a bridge. Thus, these two hypotheses, assuming either a more fluid or solid character of glial cells, are mutually exclusive. Nevertheless, both of them are still widely accepted, despite the fact that they must be considered mere speculations. There is a nearly complete lack of data on glial cell mechanics because current glial cell research has been focused on their electrophysiological and biochemical properties.

Recently, it has been shown that neurons are capable of sensing the stiffness of their environment *in vitro* and prefer soft

substrates (3). However, little is known about the mechanical properties of their physiological environment, i.e., particularly the glial cells that fill most of the space between the neuronal elements. Interestingly, glial cells *in vitro* grow better on hard materials (4). Rheological studies on brainstem preparations have been carried out to understand posttraumatic alterations in tissue of the CNS (5). However, even the normal mechanical properties at the level of individual neural cells are still poorly understood. For the retina as an ontogenetically evolved part of the CNS, biomechanics may play an especially important role. This thin, fragile tissue sheet is held in place by a subtle balance between the intraocular pressure and suction from retinal pigment epithelium (6). Several retinal disorders such as retinoschisis, malignant myopia, and retinal detachment are thought to be caused by mechanical stress facilitated by anomalous mechanical properties of retinal (glial) cells (7).

Results

We assessed the mechanical properties of both neurons and glial cells from two different areas of the mammalian CNS, the hippocampus (a part of the brain) and the retina. As representative cell “pairs” of the two tissues, we investigated (i) pyramidal neurons and astrocytes (glial cells) of the hippocampus, and (ii) retinal interneurons (i.e., bipolar and amacrine cells) and Müller (glial) cells. To characterize the local viscoelastic properties of individual cells, we measured the complex Young’s modulus $E^* = E' + iE''$ in a defined range of deforming frequencies (30, 100, and 200 Hz) using a scanning force microscope (SFM) (8, 9). A detailed frequency scan of Müller cells is shown in Fig. 5, which is published as supporting information on the PNAS web site. The real part E' reflects the elastic storage (energy storage) response and the imaginary part E'' reflects the viscous loss (energy dissipation) response of the tissue. Thus, the resulting storage modulus is a measure of a tissue’s elastic stiffness and the loss modulus measures the tissue’s viscous properties. Furthermore, we measured the Poisson’s ratio ν , which describes the tendency of a material to contract in two dimensions when it is stretched in the third one (Fig. 6, which is published as supporting information on the PNAS web site). In the case of both types of CNS tissues studied, all of the enzymatically acutely dissoci-

Author contributions: Y.-B.L. and K.F. contributed equally to this work; K.F., P.J., J.K., and A.R. designed research; Y.-B.L., K.F., and H.W. performed research; G.S., C.S., F.K., J.G., and E.-Q.W. contributed new reagents/analytic tools; Y.-B.L. and K.F. analyzed data; and K.F., J.K., and A.R. wrote the paper.

The authors declare no conflict of interest.

This article is a PNAS direct submission.

Abbreviations: SFM, scanning force microscope(microscopy); ACSF, artificial cerebrospinal fluid.

^{§§}To whom correspondence should be addressed. E-mail: jkaes@physik.uni-leipzig.de.

© 2006 by The National Academy of Sciences of the USA

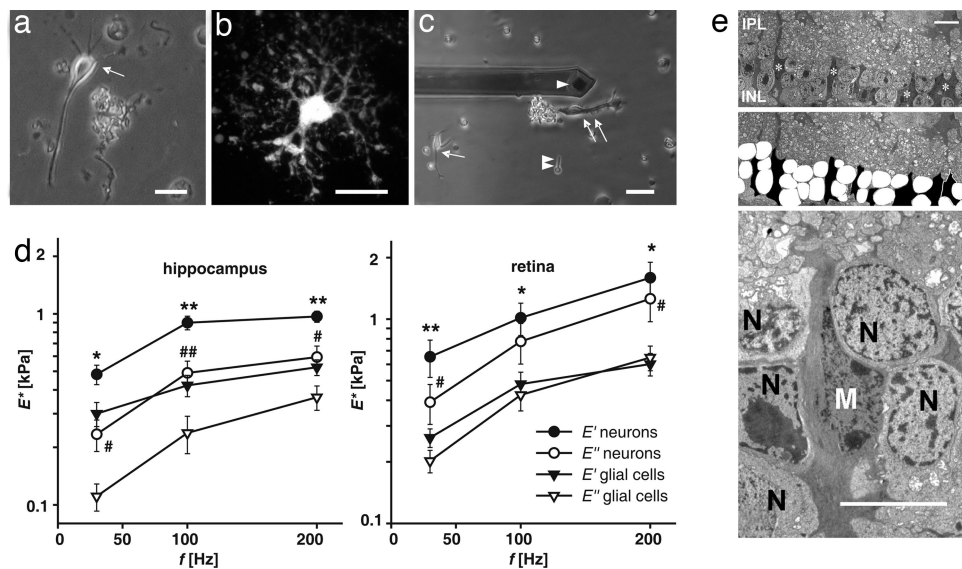


Fig. 1. Comparison of viscoelastic properties of neurons and glial cells. (a–c) Acutely dissociated cells from hippocampus (a, arrow, pyramidal neuron; b, GFAP-EGFP-fluorescent astrocyte) and retina (c, single arrow, bipolar neuron; double arrow, Müller glial cell; double arrowhead, photoreceptor cell) are shown. The tip of the cantilever is also visible in c (single arrowhead). (a and c) Phase-contrast images. (b) Fluorescence image. (d) Elastic storage (E') and viscous loss modulus (E'') of somata of hippocampal ($n = 43$) and retinal (bipolar cells, $n = 6$; amacrine cells, $n = 5$) neurons and glial cells (hippocampal astrocytes, $n = 40$; retinal Müller cells, $n = 40$) (mean \pm SEM) is shown. In both types of CNS tissues, glial cells are softer than neurons because E'_{glia} is statistically significant smaller than E'_{neuron} (*, $P < 0.05$; **, $P < 0.01$, E'_{neurons} vs. E'_{glia} ; #, $P < 0.05$; ##, $P < 0.01$, E'_{neurons} vs. E'_{glia}), and for all cell types $E'/E'' > 1$, which means that they have an all-over elastically restoring force. (e) (Top) Transmission electron micrograph of the inner nuclear layer (INL) of a guinea pig retina, close to the optic disk. Asterisks indicate Müller cell somata. (Middle) The same image; in the INL, neuronal cell somata are labeled in white, Müller cell somata are in black. Note the more irregular outline of the latter. (Bottom) The image at higher magnification. IPL, inner plexiform layer; M, Müller cell nucleus; N, nuclei of retinal interneurons. (Scale bars: a–c, 20 μm ; e, 10 μm .)

ated cells remained vital during measurement, and most even maintained their characteristic morphology (Fig. 1 a–c).

Two general features became obvious. First, in all evaluated cell types the elastic response was dominant as compared with the viscous response (i.e., E' was greater than E''). Thus, CNS cells displayed the rheological characteristics of elastic solids. Second, glial cells were found to be about twice as soft as neurons.

A detailed comparison between neurons (pyramidal cells) and glial cells (astrocytes) from the hippocampus revealed distinct differences. As shown in Fig. 1d, the elastic storage modulus E' and the viscous loss modulus E'' of neurons were significantly higher than corresponding values of glial cells. The somata of pyramidal neurons had an elastic modulus between ≈ 480 Pa at 30 Hz and ≈ 970 Pa at 200 Hz. E' of astrocyte somata was between ≈ 300 Pa at 30 Hz and ≈ 520 Pa at 200 Hz. The same situation was found for the retina. Data from somata of retinal neurons, i.e., bipolar and amacrine cells, which displayed similar values, were compared with data from somata of Müller glial cells. The E' value of the somata of investigated neurons ranged from ≈ 650 Pa at 30 Hz to $\approx 1,590$ Pa at 200 Hz; that of the somata of Müller glial cells was between ≈ 260 Pa at 30 Hz and ≈ 600 Pa at 200 Hz (Fig. 1d).

Bipolar and amacrine neurons, situated in the same retinal layer as the Müller glial cell somata, are stiffer than the latter (Fig. 1d). Because *in situ* the somata of these three cell types are closely packed together, this mechanical difference should result in different degrees of deformation. We examined this hypothesis by using electron microscopy (Fig. 1e). The cytoplasm of guinea-pig Müller cells is known to be electron-denser than that of the neurons (10), allowing an easy identification. The somata of bipolar cells were smoothly rounded on average and seen to indent the neighboring, irregular-shaped Müller cell somata; this finding was consistent with our finding that Müller cells were softer.

Müller cells are typical glial cells with an extended morphology that lends itself easily to a detailed study of the spatial distribution of viscoelastic properties within individual cells.

They have a characteristic bipolar shape with two distinct stem processes emanating from the soma, one terminating in a wide endfoot and the other one in thin branches and microvilli (Fig. 2a) (11). We separately characterized the wide endfoot, densely packed with smooth endoplasmic reticulum, the adjacent inner stem process, containing mainly bundles of intermediate filaments, the bulged soma with the nucleus and the perinuclear cytoplasm, and the thin outer process, containing microtubules (12, 13). Both of the Müller cell processes were significantly softer than soma and endfoot, whereas the soma was even stiffer than the endfoot. The elastic moduli of the inner and outer processes were ≈ 130 and ≈ 100 Pa at 30 Hz and ≈ 160 and ≈ 210 Pa at 200 Hz, respectively. In comparison, we measured $\approx 220/370$ Pa at 30/200 Hz for endfeet and $\approx 260/600$ Pa at 30/200 Hz for cell somata (Fig. 2b).

The observation that cell processes were softer than the somata was also made for pyramidal neurons. Furthermore, the inner segments of photoreceptor cells proved to be softer than their somata. The storage moduli of both Müller (glial) cell and pyramidal cell processes amounted to about one-third of their respective somata, whereas the storage moduli of Müller cell endfeet and photoreceptor inner segments amounted to about two-thirds of their respective somata (Fig. 2c).

Our results show that glial cells act as soft compliant structures surrounding the neurons, which may be comparable to cushioning material in common packaging. Because this means that they could protect the neurons from mechanical trauma, we analyzed the reaction of whole glial cells to a global deformation. For this purpose we used an optical cell stretcher (Fig. 3) (14). After trapping the cells in this dual-beam infrared laser trap at low power, a 10-fold increase in the laser power led to a deforming force on the surface of the cells on the order of hundreds of piconewtons. The exact cell stretching and subsequent relaxation behavior was found to be analogous to the behavior of two Voigt elements in series (Fig. 3b). The Voigt element is a viscoelastic

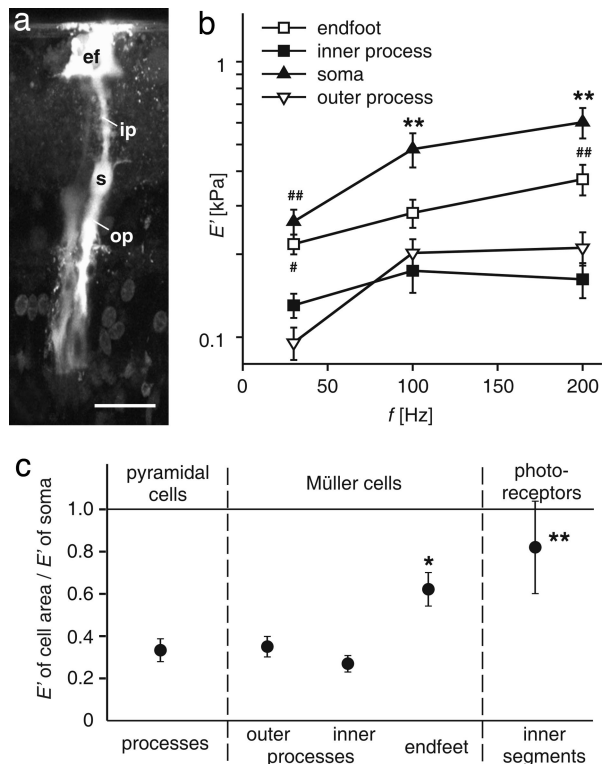


Fig. 2. Spatial variation of the cells' mechanical properties. (a) Fluorescence microphotograph of a dye-injected Müller cell (Lucifer Yellow) in a guinea pig retinal slice preparation. ef, endfoot; ip, inner process; s, soma; op, outer process of the Müller cell. (Scale bar: 20 μm .) (b) Comparison of the stiffness of different parts of the radial glial (Müller) cells of the retina (#, $P < 0.05$; ##, $P < 0.01$ vs. processes; **, $P < 0.01$ vs. all other parts of Müller cells; mean \pm SEM). Both cell processes were significantly softer than somata and endfeet, which might be attributed to a different distribution of cell organelles rather than of cytoskeletal elements. (c) Relative stiffness of the respective cellular areas compared with the soma of the according cell ($E'_{cell\ area} / E'_{soma}$) at 200 Hz (*, $P < 0.05$; **, $P < 0.01$ vs. cell processes; mean \pm SEM). Processes of Müller cells and pyramidal cells displayed a similar relative stiffness. The endfeet of Müller cells and the inner segments of photoreceptor cells were stiffer with respect to the other cellular compartments, but softer than their somata. Similar relations were observed at 30 and 100 Hz.

object composed of a restoring spring (elastic part) and a dissipative dashpot (viscous part), connected in parallel (Fig. 3b *Inset*). The resulting overdamped viscoelastic behavior of the cells is comparable to that of shock absorbers (a detailed description of the calculation is given as *Supporting Text*, which is published as supporting information on the PNAS web site).

The measurements on the cellular level were accompanied by bulk rheological measurements on slices of hippocampi and retinal wholemount preparations (Fig. 4). In analogy to the complex Young's modulus E^* we determined the complex shear modulus $G^* = G' + iG''$ [$G^* = E^*/2(1 + \nu)$], where ν is the Poisson's ratio as a function of frequency. We found that for intact tissue the elastic behavior was dominant over the whole frequency range, i.e., $G' > G''$, in agreement with our data on isolated cells. Both tissues were comparatively soft with a storage modulus not exceeding a few hundred Pascal in the case of the hippocampus (Fig. 4a) and even < 100 Pa in the case of the retina (Fig. 4b). Finally, a conversion of the mechanical storage modulus E' measured for single cells (compare Figs. 1 and 2) into the storage component of the shear modulus G' measured for tissues (compare Fig. 4a and b) revealed that the elastic moduli are of the same magnitude (Fig. 4c and d).

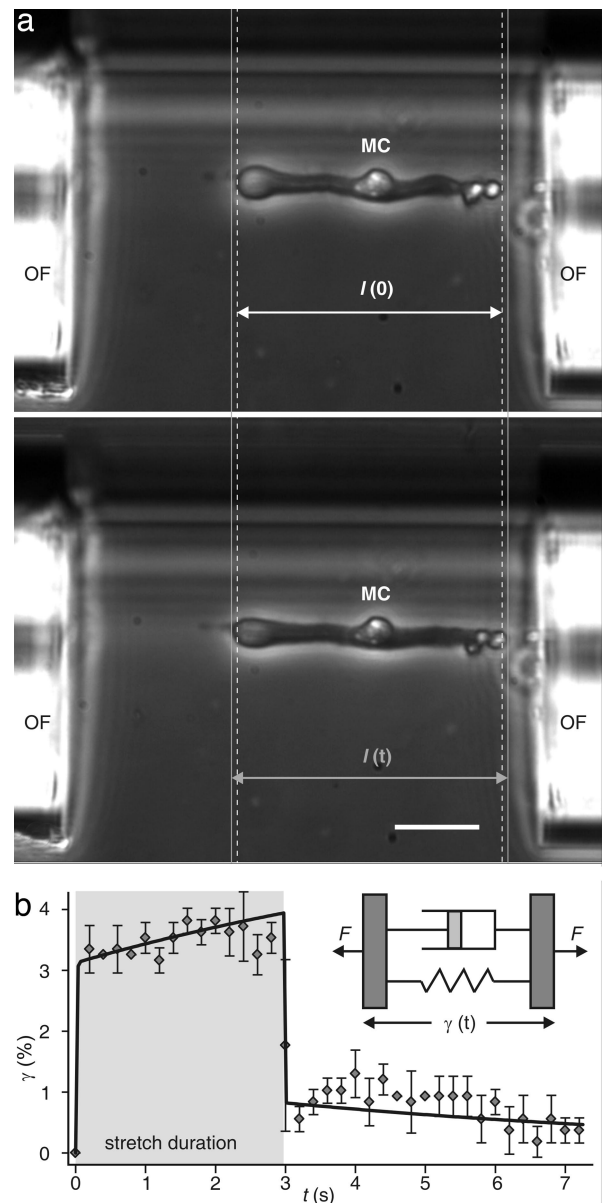


Fig. 3. Mechanical deformation and relaxation behavior of a whole Müller (glial) cell (MC) deformed with an optical stretcher. Cells with a length $l(0)$ are aligned with the forces induced on their surface by two infrared laser beams emanating from the optical fibers (OF), whose ends are visible on both sides of the image. (a *Upper*) Increasing the laser power leads to a stretching of the cells along the laser beam axes. (a *Lower*) That process results in a cell length $l(t)$. The gray lines help to compare the length before and during the stretching. (Scale bar: 25 μm .) (b) Axial cell strain $\gamma = [l(t) - l(0)] / l(0)$ as a function of time (mean \pm SD). The viscoelastic response of a stretched cell can be modeled by two viscoelastic Voigt elements in series (solid line), resembling a shock absorber. The gray area indicates the duration of the stretching. (*Inset*) The Voigt model considers a material to be composed of a spring and a dashpot connected in parallel, which represent its elastic and viscous components, respectively. F , forces acting on the viscoelastic object.

Discussion

In summary, we used SFM to study local viscoelastic properties of the CNS's principal individual building blocks, neurons and glial cells. Because the environment of cell cultures differs considerably from that existing *in vivo*, alterations of cultured cells, especially of their mechanical properties, are very likely to occur. To avoid any culture artifacts (15), our SFM measurements were performed on

these substrates neurons form significantly more branches than on stiffer ones (3, 4). This observation leads to the appealing hypothesis that the softness of glial cells facilitates neurite growth or is even a precondition during ontogenetic development and in the course of physiological (e.g., activity dependent) and pathophysiological neuronal plasticity (e.g., during neuronal regeneration). The hippocampus exhibits a particularly high degree of wiring plasticity (28) and is known to generate new neurons and glial cells throughout adulthood; the processes of the newly born cells must penetrate the adult tissue to contact target cells and become functional (29). Furthermore, extensive (anomalous) growth of neuronal cell processes has been demonstrated in the retina after cellular degeneration (30, 31); in accordance with our hypothesis, the sites of such growth (and the normal developmental establishment of synaptic contacts) are the plexiform layers where Müller cells are softest (Fig. 7, which is published as supporting information on the PNAS web site; compare Fig. 2*b*). In summary, the biomechanical properties of glial cells may enable them to perform even more neuron-supportive functions than hitherto elucidated by electrophysiological and biochemical work.

Materials and Methods

All experiments were carried out in accordance with applicable German laws of animal protection and the Association for Research in Vision and Ophthalmology Statement for the Use of Animals in Ophthalmic and Vision Research.

Sample Preparation. Retinal cells. Retinal cells of adult guinea pigs were acutely isolated as described (32). Briefly, guinea pigs were deeply anesthetized and killed by an overdose of urethane (2 g/kg, i.p.). After enucleation of the eyes and excision of the retina, retinal pieces were incubated in Ca^{2+} - and Mg^{2+} -free PBS (pH 7.4; Seromed Biochrom, Berlin, Germany) containing papain (0.03–0.1 mg/ml; Boehringer Mannheim, Mannheim, Germany) for 30 min at room temperature or at 37°C. After washing with PBS containing DNase I (200 units/ml; Sigma, Deisenhofen, Germany), the tissue pieces were gently triturated by a wide-bore pipette to obtain suspensions of isolated cells. The cell suspensions were stored at 4°C up to 4 h (33) in extracellular solution until use. The main retinal cell types found in the suspensions (amacrine cells, bipolar cells, photoreceptor cells, and Müller glial cells) were easily distinguished by their morphology (compare Fig. 1*a*).

Extracellular solution consisted of 136 mM NaCl, 3 mM KCl, 1 mM MgCl_2 , 10 mM Hepes, 2 mM CaCl_2 , and 10 mM D-glucose. The pH of the solution was adjusted to 7.4 by using Tris (1 M; pH 10.42). **Hippocampal cells.** Cells were acutely isolated as described (34, 35). Briefly, Tg(hGFAP/EGFP) mice (36) from postnatal days 25–30 were decapitated, and their brains were dissected and cut into 300- μm -thick slices in frontal orientation by using a vibratome (HM 650V; Microm International, Walldorf, Germany). Slice preparation was performed in ice-cold, carbogen-saturated (95% O_2 /5% CO_2) artificial cerebrospinal fluid (ACSF) containing sucrose (pH 7.4). After incubation for 30 min at 35°C in ACSF containing sucrose, the slices were stored for 20 min in ACSF at room temperature. Then the slices were incubated for 12–15 min either in pronase- (2 mg/ml; Roche, Indianapolis, IN) or papain-containing solution (2 mg/ml, supplemented with 0.3 mg/ml L-cysteine; Sigma) at room temperature for the isolation of neurons and glial cells, respectively. After washing, the CA1 region of the hippocampus was dissected, and cells were isolated in Hepes-buffered solution by using wide-bore pipettes. The cell suspensions contained many pyramidal neurons (identified by their characteristic morphology) and astrocytes (identified by their inherent EGFP fluorescence).

ACSF with sucrose consisted of 87 mM NaCl, 2.5 mM KCl, 1.25 mM NaH_2PO_4 , 7 mM MgCl_2 , 0.5 mM CaCl_2 , 25 mM NaHCO_3 , 25 mM D-glucose, and 75 mM sucrose gassed with 95% O_2 /5% CO_2 .

ACSF without sucrose consisted of 126 mM NaCl, 3 mM KCl, 1.25 mM NaH_2PO_4 , 2 mM MgSO_4 , 2 mM CaCl_2 , 26 mM NaHCO_3 , and 10 mM D-glucose gassed with 95% O_2 /5% CO_2 .

Hepes-buffered solution consisted of 150 mM NaCl, 5 mM KCl, 2 mM MgSO_4 , 2 mM CaCl_2 , 10 mM Hepes, and 10 mM D-glucose; gassed with 100% O_2 . The pH of the solution was adjusted to 7.4 by using NaOH or HCl.

Tissue slices. Fresh bovine eyeballs and brains were obtained from a local slaughterhouse and stored in ice-cold PBS. Retinae and hippocampi were excised immediately before the experiments. Circular retinal pieces were obtained by using a stamp-like tool; hippocampal pieces were first “stamped out,” and subsequently sliced with a scalpel blade.

Electron Microscopy. Excised guinea pig eyes were opened at their corneal margin, the vitreous body was removed, and the eyecups were then fixed in a buffered mixture of 0.5% glutaraldehyde and 4% paraformaldehyde overnight and postfixed in 1% osmium tetroxide for 2 h. Subsequently, eyecups were rinsed and dehydrated in ethanol. The tissue was stained overnight in 70% ethanol saturated with uranylacetate. After further dehydration in absolute ethanol and propylene oxide, the samples were embedded in a Araldite 502 Kit (Sigma) and sectioned on a Reichert FCR Ultracut ultramicrotome (Leica, Bensheim, Germany). Ultrathin sections were stained with uranylacetate and lead citrate, and then studied by using an EM 10 electron microscope (Zeiss, Oberkochen, Germany).

Biophysical Measurements. SFM. SFM measurements were taken with a NanoWizard SFM (JPK Instruments, Berlin, Germany), which was placed on an inverted microscope DM IRB (Leica Microsystems, Wetzlar, Germany). Commercial cantilevers (NANOSENSORS; Nano World, Schaffhausen, Switzerland) with spring constants of ≈ 0.02 – 0.06 N/m were modified as described (8, 9) by gluing polystyrene beads (Seradyn Particle Technology, Indianapolis, IN; radius ≈ 3 μm) to the tip, to avoid damage of the sample and any nonlinear deforming stresses. The oscillatory drive signal necessary to perform frequency-dependent viscoelasticity measurements was fed to the scanner signal through a lock-in amplifier SR850 (Stanford Research Systems, Sunnyvale, CA) (8). Phase and amplitude differences between the applied modulation and the cantilever response signal were recorded. Cells were placed on commercial glass slides, Superfrost-Plus (Menzel-Gläser, Braunschweig, Germany). A detailed description of the force measurements on acutely isolated cells is published as *Supporting Text*.

Bulk rheology. Circular pieces of 25- and 8-mm diameter were cut out of bovine retinal whole mounts and hippocampal slices, respectively. These pieces were then placed on a RFS 3 Rheometer (Scientific Rheometric, Piscataway, NJ). Subsequently, a stainless-steel plate of according size was brought into contact with the upper surface of the tissue. The adhesion of the tissues to the steel plates was strong for frequencies between 0.1 and 150 rad/s; in control experiments with the tissues fixed to the plates with fibrinogen/thrombin gels similar results were obtained. The frequency sweeps, i.e., examination of G' and G'' at different frequencies, were carried out with controlled applied strain of 2%.

Optical stretcher. Isolated guinea pig Müller cells were trapped and aligned in a dual beam infrared laser trap ($\lambda = 1,064$ nm) which was mounted on an inverted microscope (DMIL, Leica) (trapping power 0.1 W in each beam). Increasing the laser power (1.0 W) led to a stretching of the cells along the laser axis (14, 19, 37). Cells were recorded with a digital camera (Basler A202k; Basler Vision, Ahrensburg, Germany). Changes in cell length were obtained by using custom-built software (based on LabView, National Instruments, Austin, TX), and data analysis was done by using Igor Pro (WaveMetrics, Lake Oswego, OR) software.

We thank Peter Rudolf (Institut für Klassische Philologie und Komparatistik, Universität Leipzig) for inspiring discussions about the terminology of glia; Jens Grosche and Katja Rillich for providing images; and Bernd Kohlstrunk for technical help. This study was supported by a stipend from the Deutscher Akademischer Austausch-

chdienst through the Sandwich Program (to Y.-B.L.), Deutsche Forschungsgemeinschaft Research Training School "InterNeuro" Grant GRK 1097 (to J.K. and A.R.), and Deutsche Forschungsgemeinschaft Priority Program "Glia and Synapse" Grant SPP 1172 (to G.S., C.S., F.K., and A.R.).

1. Virchow R (1856) *Gesammelte Abhandlungen zur Wissenschaftlichen Medicin* (von Meidinger Sohn, Frankfurt, Germany).
2. Schultze M (1866) *Zur Anatomie und Physiologie der Retina* (von Max Cohen & Sohn, Bonn, Germany).
3. Flanagan LA, Ju YE, Marg B, Osterfield M, Janmey PA (2002) *NeuroReport* 13:2411–2415.
4. Georges PC, Miller WJ, Meaney DF, Sawyer E, Janmey PA (2006) *Biophys J* 90:3012–3018.
5. Arbogast KB, Margulies SS (1998) *J Biomech* 31:801–807.
6. Yao XY, Hageman GS, Marmor MF (1994) *Invest Ophthalmol Visual Sci* 35:744–748.
7. Reid SN, Yamashita C, Farber DB (2003) *J Neurosci* 23:6030–6040.
8. Mahaffy RE, Shih CK, MacKintosh FC, Kas J (2000) *Phys Rev Lett* 85:880–883.
9. Mahaffy RE, Park S, Gerde E, Kas J, Shih CK (2004) *Biophys J* 86:1777–1793.
10. Germer A, Biedermann B, Wolburg H, Schuck J, Grosche J, Kuhrt H, Reichelt W, Schousboe A, Paasche G, Mack AF, Reichenbach A (1998) *J Neurocytol* 27:329–345.
11. Reichenbach A, Schneider H, Leibnitz L, Reichelt W, Schaaf P, Schumann R (1989) *Anat Embryol (Berl)* 180:71–79.
12. Reichenbach A, Hagen E, Schippel K, Bruckner G, Reichelt W, Leibnitz L (1988) *Z Mikrosk Anat Forsch* 102:897–912.
13. Reichenbach A, Hagen E, Schippel K, Eberhardt W (1988) *Z Mikrosk Anat Forsch* 102:721–755.
14. Guck J, Ananthakrishnan R, Mahmood H, Moon TJ, Cunningham CC, Kas J (2001) *Biophys J* 81:767–784.
15. Guidry C (1996) *Invest Ophthalmol Visual Sci* 37:740–752.
16. Moore SW, Keller RE, Koehl MA (1995) *Development (Cambridge, UK)* 121:3131–3140.
17. Vaughan DK, Fisher SK (1987) *Exp Eye Res* 44:393–406.
18. Rotsch C, Radmacher M (2000) *Biophys J* 78:520–535.
19. Wottawah F, Schinkinger S, Lincoln B, Ananthakrishnan R, Romeyke M, Guck J, Kas J (2005) *Phys Rev Lett* 94:098103.
20. Ananthakrishnan R, Guck J, Wottawah F, Schinkinger S, Lincoln B, Romeyke M, Moon T, Kas J (2006) *J Theor Biol* 242:502–516.
21. Caille N, Thoumine O, Tardy Y, Meister JJ (2002) *J Biomech* 35:177–187.
22. Leduc C, Campas O, Zeldovich KB, Roux A, Jolimaitre P, Bourel-Bonnet L, Goud B, Joanny JF, Bassereau P, Prost J (2004) *Proc Natl Acad Sci USA* 101:17096–17101.
23. Discher DE, Janmey P, Wang YL (2005) *Science* 310:1139–1143.
24. Bilston LE, Liu Z, Phan-Thien N (1997) *Biorheology* 34:377–385.
25. Czosnyka M, Pickard JD (2004) *J Neurol Neurosurg Psychiatry* 75:813–821.
26. Martin XD (1992) *Ophthalmologica* 205:57–63.
27. Uckermann O, Vargova L, Ulbricht E, Klaus C, Weick M, Rillich K, Wiedemann P, Reichenbach A, Sykova E, Bringmann A (2004) *J Neurosci* 24:10149–10158.
28. Pittenger C, Kandel ER (2003) *Philos Trans R Soc London B* 358:757–763.
29. Ming GL, Song H (2005) *Annu Rev Neurosci* 28:223–250.
30. Peichl L, Bolz J (1984) *Science* 223:503–504.
31. Lewis GP, Sethi CS, Linberg KA, Charteris DG, Fisher SK (2003) *Mol Neurobiol* 28:159–175.
32. Francke M, Weick M, Pannicke T, Uckermann O, Grosche J, Goczalik I, Milenkovic I, Uhlmann S, Faude F, Wiedemann P, et al. (2002) *Invest Ophthalmol Visual Sci* 43:870–881.
33. Gefen A, Margulies SS (2004) *J Biomech* 37:1339–1352.
34. Weber M, Dietrich D, Grasel I, Reuter G, Seifert G, Steinhauser C (2001) *J Neurochem* 77:1108–1115.
35. Matthias K, Kirchhoff F, Seifert G, Huttmann K, Matyash M, Kettenmann H, Steinhauser C (2003) *J Neurosci* 23:1750–1758.
36. Nolte C, Matyash M, Pivneva T, Schipke CG, Ohlemeyer C, Hanisch UK, Kirchhoff F, Kettenmann H (2001) *Glia* 33:72–86.
37. Guck J, Ananthakrishnan R, Moon TJ, Cunningham CC, Kas J (2000) *Phys Rev Lett* 84:5451–5454.